THE JOURNAL OF BIOLOGICAL CHEMISTRY VOL. 290, NO. 4, pp. 2321–2333, January 23, 2015

Phosphorylation and Inactivation of Glycogen Synthase Kinase 3β (GSK3β) by Dual-specificity Tyrosine Phosphorylation-regulated Kinase 1A (Dyrk1A)*

Received for publication, July 8, 2014, and in revised form, November 14, 2014 Published, JBC Papers in Press, December 4, 2014, DOI 10.1074/jbc.M114.594952

Woo-Joo Song[‡§], Eun-Ah Christine Song[‡§], Min-Su Jung[§], Sun-Hee Choi[§], Hyung-Hwan Baik[‡], Byung Kwan Jin[‡], Jeong Hee Kim[¶‖], and Sul-Hee Chung[‡§1]

From the [‡]Department of Biochemistry and Molecular Biology, Neurodegeneration Control Research Center, School of Medicine, [¶]Department of Oral Biochemistry and Molecular Biology, School of Dentistry, and [‖]Department of Life and Nanopharmaceutical Sciences, Kyung Hee University, Seoul 130-701, Korea and the [§]Institute for Brain Science and Technology, Inje University, Busan 614-735, Korea

Background: The regulatory mechanism of GSK3β activity is not yet fully understood.
Results: Dyrk1A inactivates GSK3β by phosphorylation at Thr^{356}, which may contribute to an obesity-resistant phenotype.
Conclusion: Dyrk1A-mediated phosphorylation is an alternative pathway for GSK3β inactivation.
Significance: Understanding the mechanism regulating GSK3β activity is crucial for developing new therapies against GSK3β-associated diseases, including obesity.

Glycogen synthase kinase 3β (GSK3β) participates in many cellular processes, and its dysregulation has been implicated in a wide range of diseases such as obesity, type 2 diabetes, cancer, and Alzheimer disease. Inactivation of GSK3β by phosphorylation at specific residues is a primary mechanism by which this constitutively active kinase is controlled. However, the regulatory mechanism of GSK3β is not fully understood. Dual-specificity tyrosine phosphorylation-regulated kinase 1A (Dyrk1A) has multiple biological functions that occur as the result of phosphorylation of diverse proteins that are involved in metabolism, synaptic function, and neurodegeneration. Here we show that GSK3β directly interacts with and is phosphorylated by Dyrk1A. Dyrk1A-mediated phosphorylation at the Thr^{356} residue inhibits GSK3β activity. Dyrk1A transgenic (TG) mice are lean and resistant to diet-induced obesity because of reduced fat mass, which shows an inverse correlation with the effect of GSK3β on obesity. This result suggests a potential *in vivo* association between GSK3β and Dyrk1A regarding the mechanism underlying obesity. The level of $Thr(P)^{356}$-GSK3β was higher in the white adipose tissue of Dyrk1A TG mice compared with control mice. GSK3β activity was differentially regulated by phosphorylation at different sites in adipose tissue depending on the type of diet the mice were fed. Furthermore, overexpression of Dyrk1A suppressed the expression of adipogenic proteins, including peroxisome proliferator-activated receptor γ, in 3T3-L1 cells and in young Dyrk1A TG mice fed a chow diet. Taken together, these results reveal a novel regulatory mechanism for GSK3β activity and indicate that overexpression of Dyrk1A may contribute to the obesity-resistant phenotype through phosphorylation and inactivation of GSK3β.

Glycogen synthase kinase 3 (GSK3), which consists of the highly homologous GSK3α and GSK3β, is constitutively active in unstimulated cells under normal circumstances. Therefore, inactivation of GSK3β through phosphorylation at specific residues is a key control mechanism for GSK3β activity. Phosphorylation at Ser^9 of GSK3β is mediated by Akt and other kinases and is the most common mechanism of GSK3β inactivation (1, 2), although phosphorylation at Ser^{389} by p38 MAPK is another pathway for GSK3β inactivation (3). GSK3β is a multifunctional serine/threonine protein kinase that regulates numerous cellular processes such as metabolism, signaling pathways, apoptosis/cell survival, and development. As a result of these various roles, dysregulation of GSK3β has been implicated in the pathogenesis of several human diseases, including obesity, diabetes, cancer, and Alzheimer disease (AD)[2] (4, 5). Therefore, understanding the regulatory mechanism of GSK3β activity is important for the development of potential drugs that might slow or halt the progression of these diseases.

Dual-specificity tyrosine phosphorylation-regulated kinase 1A (Dyrk1A) is a proline-directed serine/threonine kinase that might be responsible for several pathological phenotypes, including mental retardation and early onset AD in Down syndrome patients. Dyrk1A is implicated in various biological pathways by phosphorylation of diverse substrate proteins such as transcription factors, splicing factors, and synaptic proteins (6). Dyrk1A KO mice display fetal developmental delays and are

* This work was supported by Korea Healthcare Technology R&D Project, Ministry of Health, Welfare and Family Affairs, Republic of Korea Grant A092004 and by the Basic Science Research Program through the National Research Foundation (NRF) of Korea funded by the Ministry of Education, Science and Technology (Grants 2011-0014085, 2011-0023401, 2012R1A1A2040129, 2011-0030072, and 2012-0000495). This work was also supported by the National Research Foundation of Korea (NRF) grant funded by the Korea government (MSIP) (No. 2008-0061888).

[1] To whom correspondence should be addressed: Kyung Hee University, School of Medicine, #1 Hoegi-dong, Dongdaemoon-gu, Seoul 130-701, Korea. Tel.: 82-2-961-0317; Fax: 82-2-961-4570; E-mail: sulchung@khu.ac.kr or sulchung2@gmail.com.

[2] The abbreviations used are: AD, Alzheimer disease; TG, transgenic; PPAR, peroxisome proliferator-activated receptor; IP, immunoprecipitation; NFAT, nuclear factor of activated T cells; HFD, high-fat diet; WAT, white adipose tissue.

embryonic lethal, indicating that there is fundamental physiological importance of Dyrk1A (7). Transgenic (TG) mice that overexpress Dyrk1A (Dyrk1A TG mice) show learning and memory defects (8, 9). Overexpression of Dyrk1A may contribute to early onset AD through hyperphosphorylation of Tau and increased Aβ production via phosphorylation of amyloid precursor protein and presenilin 1 (10–13).

Obesity is a condition that is characterized by excessive fat accumulation in the body. Obesity is a major public health problem that has been rapidly increasing worldwide and is associated with metabolic disorders such as type 2 diabetes, hypertension, heart disease, and cancer. GSK3β TG mice that overexpressed human GSK3β in the skeletal muscle displayed body weight gain because of an increase in fat mass (14). In this study, we show that Dyrk1A inactivates GSK3β by direct phosphorylation at the Thr^{356} residue. Dyrk1A TG mice exhibit a lean phenotype and have reduced fat content. This could be attributed to the opposite effect of GSK3β and Dyrk1A on body weight and fat content. These results led us to examine a functional association between GSK3β and Dyrk1A in the mechanism of obesity. Our results reveal that phosphorylation by Dyrk1A is a novel pathway for GSK3β inactivation and that it has a potentially important role in the mechanism of obesity.

EXPERIMENTAL PROCEDURES

Proteins and Antibodies—Mouse WT and Y321F kinase-inactive mutant Dyrk1A proteins with endogenous 13-histidine repeats were purified with nickel-nitrilotriacetic acid resin as described previously (11). Full-length mouse GSK3β and mutants were cloned into pET25b or pGEX4T-3 for protein purification. The recombinant proteins were expressed in the *Escherichia coli* BL21(DE3) RIL strain (Stratagene) and purified using nickel-nitrilotriacetic acid or glutathione-Sepharose 4B resin.

The anti-Dyrk1A antibody was either purchased from Santa Cruz Biotechnology or custom-made as described previously (9). A phosphospecific GSK3β (Thr(P)^{356}-GSK3β) antibody to a synthetic phosphopeptide (^{352}NGRDpTPALFN^{361}) was generated and affinity-purified first with a cognate non-phosphopeptide (NGRDTPALFN) affinity column and then with a phosphopeptide column (Peptron, Korea). The antibodies for GSK3β, Ser(P)^{9}-GSK3β, Ser(P)^{641}-glycogen synthase (GS), GS, β-catenin, fatty acid binding protein 4 (FABP4, also called adipocyte protein 2 (aP2)), peroxisome proliferator-activated receptor γ (PPARγ), and CCAAT/enhancer binding protein α (C/EBPα) were purchased from Cell Signaling Technology. Anti-c-myc and α-tubulin antibodies were obtained from Sigma, and anti-GAPDH antibody was purchased from Santa Cruz Biotechnology. The phosphospecific GSK3β (Ser(P)^{389}-GSK3β) and phosphospecific Tau (pT212-Tau) antibodies were obtained from Millipore and BIOSOURCE, respectively. Anti-Tau and anti-GST antibodies were purchased from Invitrogen and AbFrontier, respectively.

Plasmids and siRNAs—The full-length wild-type and Y321F kinase-inactive Dyrk1A mutant cDNAs were cloned into pcDNA3.1 (Invitrogen) as described previously (11). The full-length mouse GSK3β cDNA was cloned into pcDNA3.1. Mutants of GSK3β cDNA were generated by DpnI-mediated site-directed mutagenesis (Stratagene), and the clones were verified by sequencing. Mouse full-length GS in pCMV Sport 6 was obtained from the Korea Human Gene Bank, and the β-catenin in pEGFP-C1 vector was provided by Dr. Kwonseop Kim (Chonnam National University, Korea).

For the siRNA experiment, the Dyrk1A-specific siRNA (5′-AUGGAGCUAUGGACGUUAA) with the TT overhang was synthesized by ST Pharm. Co. One day before transfection, 3T3-L1 cells (1×10^5 cells/60-mm plate) were plated in DMEM with 10% FBS, followed by duplex siRNA transfection (100 nM) using X-tremeGENE transfection reagents (Roche). After 48 h of siRNA treatment, cell lysates were prepared for immunoblot analyses.

In Vitro Kinase Assays—In vitro kinase assays for Dyrk1A were carried out as described previously (15). For analysis by autoradiography, purified GSK3β wild-type (WT), K85R, or mutant protein was incubated with Dyrk1A WT or Y321F inactive mutant protein for 1–1.5 h at 37 °C in kinase buffer (50 mM Tris (pH 8.0), 10 mM $MgCl_2$, 0.1 mM $CaCl_2$, 1 mM DTT, and 20 μM sodium orthovanadate) containing 10 μM cold ATP and 5 μCi [γ-^{32}P]ATP. The reaction mixtures were separated on SDS-polyacrylamide gels, and radioactive bands were detected with the Typhoon 9200 imaging system (Amersham Biosciences Pharmacia). *In vitro* GSK3β kinase assays were performed by incubating purified GSK3β WT or mutant protein at 37 °C for 10 min in kinase buffer supplemented with 50 μM ATP and a synthetic glycogen-synthase-derived (GSM) GSK3 substrate peptide (50 μM) (Upstate) using a Kinase Glo® luminescent kinase assay (Promega).

To determine the effect of Dyrk1A-mediated phosphorylation of GSK3β on its kinase activity, purified GST-GSK3β bound to glutathione-Sepharose beads was incubated with and without Dyrk1A in the presence and absence of 10 mM nonradioactive ATP at 37 °C for 1 h. The bead-bound GST fusion proteins were washed with 200 mM NaCl-containing binding buffer to remove recombinant kinase and ATP before performing the kinase assay as described above.

Coimmunoprecipitation (Co-IP) and GST Pulldown Assay—Co-IP and the GST pulldown assay were performed as described previously (16). For co-IP, brain lysates (3 mg) from Dyrk1A TG mice or lysates of HEK293T cells (500 μg) transfected with the indicated plasmids were incubated with control IgG (R&D Systems), anti-GSK3β, or anti-Dyrk1A antibodies overnight at 4 °C in ristocetin-induced platelet agglutination (RIPA) buffer (50 mM Tris (pH 8.0), 150 mM NaCl, 1% Nonidet P-40, 0.1% SDS, and 0.5% deoxycholic acid) with protease/phosphatase inhibitors and 1 mM PMSF. The next day, after 1 h of incubation with protein A beads (Pierce), the bead mixture was gently washed with RIPA buffer containing 1% Triton X-100, and the bound proteins were subjected to immunoblot analysis with the indicated antibodies. For the GST pulldown assay, purified GST-GSK3β WT was incubated with recombinant Dyrk1A protein (1 μg) for 1 h at 4 °C in 50 mM NaCl-containing binding buffer (50 mM Tris (pH 8.0), 10% glycerol, 2 mM β-mercaptoethanol, 0.01% Nonidet P-40, 0.5 mM EDTA, and 1 mM PMSF) and washed with 300 mM NaCl-containing binding buffer. The beads were then washed with 300 mM NaCl-containing bind-

ing buffer, and the bound proteins were subjected to immunoblot analysis with the indicated antibodies.

Nuclear Factor of Activated T Cells (NFAT) Luciferase Assay—Luciferase assays were performed as described previously (16). HEK293T cells were first grown in 24-well plates and then transfected with 0.5 ng pCMV-RL reporter (*Renilla* luciferase, internal standard), 200 ng of pGL3-Basic reporter (NFAT-luciferase, AP-1 promoter), and indicated amounts of expression plasmids encoding empty vector, GSK3β WT, or the phosphorylation-defective mutants. The total amount of plasmid was kept constant for all groups. After transfection, cells were treated with ionomycin (2.5 μM) for 48 h and analyzed for reporter gene activity using the Dual-Luciferase reporter assay (Promega) as recommended by the manufacturer. NFAT luciferase values were normalized to *Renilla* luciferase values.

Cell Culture and Differentiation—3T3-L1 preadipocytes were maintained and differentiated as described previously (17). For differentiation, 2-day postconfluent 3T3-L1 cells (day 0) were incubated in DMEM containing 10% FBS, 1 μM dexamethasone, 10 μg/ml insulin, and 0.5 mM 3-isobutyl-1-methylxanthine for 2 days. Cells were then cultured in DMEM containing 10% FBS and insulin for another 2 days, followed by changing with fresh DMEM containing 10% FBS every subsequent 2 days.

3T3-L1 cells were transfected with pcDNA3.1 myc-His or Dyrk1A cDNA plasmids using Lipofectamine 2000 (Invitrogen) and selected in growth medium containing 500 μg/ml G418 (Invitrogen). The G418-selected cells were then differentiated for 8 days and subjected to Oil Red O staining. Alternatively, Dyrk1A cDNA was cloned into a lentiviral vector, pLenti-suCMV (GenTarget Inc.), for lentivirus production. HEK293T cells were transfected with Lipofectamine 2000 using 5 μg of pLenti-suCMV-plasmid with 6 μg of packaging plasmid from Origene (Rockville, MD). After 48 h, lentiviruses were harvested and concentrated using Lenti-X concentrator (Clontech, Mountain View, CA), followed by infection of 3T3-L1 preadipocytes in the presence of 8 μg/ml Polybrene overnight at 37 °C. The next day, fresh DMEM-calf serum medium was added to promote continuous growth. After 2 days, cells were placed under blasticidin selection (10 μg/ml), and expression of Dyrk1A and other proteins was analyzed by Western blotting.

Mice—Dyrk1A TG mice that overexpress the human Dyrk1A gene, which was introduced using a bacterial artificial chromosome, were produced and maintained in the C57BL/6 background as described previously (9). All experiments were performed in accordance with guidelines set forth by the Inje University council directive for the proper care and use of laboratory animals. The mice were maintained in a temperature-controlled room under a light-dark cycle of 12:12 h. Five- or six-week-old mice were fed a high-fat diet (HFD, Dyets Inc.) or a normal chow diet (Purina). Food intake and body weight were measured once per week. Energy expenditure was calculated from the gas exchange data (energy expenditure = $(3.815 + 1.232 \times RQ) \times V_{O2}$), where RQ is the ratio of V_{CO2} to V_{O2}. Energy expenditure values were observed for 2 days and averaged over a 24-h period by normalizing to body weight. MRI experiments were performed on a 4.7 T animal MRI scanner (BioSpec 47/40, Bruker) with a 72-mm volume coil at the Korea Basic Science Institute (Ochang, Korea). The epididymal fat pads were embedded in paraffin, sectioned at a thickness of 7 μm, and stained with H&E for the histological examination of lipid droplets.

Preparation of Cell and Tissue Lysates and Western Blot Analysis—Preparation of lysates from cell cultures and tissues and Western blot analysis were performed as described previously (16). Mouse embryonic fibroblast WT and GSK3β ($^{-/-}$) cells were provided by Dr. Jim Woodgett (University of Toronto, Canada). HEK293T cells were transiently transfected with the indicated plasmids using the calcium phosphate precipitation method. One day after transfection, the harvested cells were lysed in RIPA buffer containing 1 mM PMSF, a protease inhibitor mixture (GenDEPOT), and a phosphatase-inhibitor mixture (GenDEPOT) and were then subjected to Western blot analysis. Mouse tissues were dissected, snap-frozen in liquid nitrogen, and Dounce-homogenized in RIPA buffer containing 1 mM PMSF, a protease inhibitor mixture, and a phosphatase inhibitor mixture. Protein concentration was determined using the BCA assay (Sigma). Typically, 25–100 μg of the cell and tissue lysates was used for Western blotting. Densitometric quantification of the immunoblots was performed using ImageJ 1.42 software (NIH).

Statistical Analysis—All statistical data are presented as the mean ± S.E. Unless stated otherwise, differences between groups were analyzed using two-tailed Student's *t* tests for comparison of two groups or by analysis of variance for comparison of more than two groups. Analyses of variance were followed by Bonferroni post hoc tests for multiple pairwise comparisons. The threshold for significance was set at $p < 0.05$.

RESULTS

Dyrk1A Interacts with GSK3β and Phosphorylates GSK3β at the Thr^{356} Residue—To determine whether GSK3β interacts with Dyrk1A, co-IP assays were performed with the lysates of HEK293T cells transfected with plasmids encoding GSK3β and Dyrk1A. Dyrk1A was immunoprecipitated with the anti-GSK3β antibody (Fig. 1*A*), and GSK3β was immunoprecipitated with the anti-Dyrk1A antibody (Fig. 1*B*), which indicates an interaction between Dyrk1A and GSK3β. To further examine the endogenous interaction of GSK3β and Dyrk1A, mouse brain lysates were immunoprecipitated with the anti-Dyrk1A antibody. Fig. 1*C* shows that Dyrk1A interacts with GSK3β in mouse brain lysates. The direct interaction between purified Dyrk1A protein and GST-GSK3β was further determined with a GST pulldown assay, which revealed that GST-GSK3β, but not GST alone, was bound to Dyrk1A (Fig. 1*D*).

Considering that Dyrk1A interacts with GSK3β, we investigated whether GSK3β is a substrate of Dyrk1A. To determine whether Dyrk1A is able to phosphorylate GSK3β *in vitro*, a purified inactive mutant of GSK3β, K85R, was incubated with recombinant Dyrk1A WT or the inactive Dyrk1A Y321F mutant in a kinase assay buffer containing [γ-^{32}P]ATP. A band that corresponds to the molecular size of GSK3β K85R was identified by autoradiography (Fig. 2*A*) only when both Dyrk1A WT and GSK3β K85R were present, indicating that GSK3β was phosphorylated by Dyrk1A.

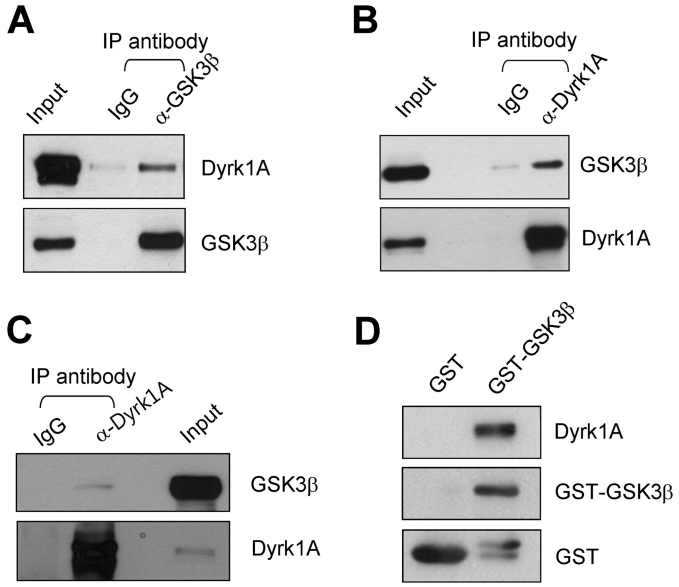

FIGURE 1. **Dyrk1A interacts with GSK3β.** *A* and *B*, co-IP assays in HEK293T cells. HEK293T cell lysates that were transfected with plasmids encoding GSK3β and Dyrk1A were immunoprecipitated with control IgG, anti-GSK3β (*A*), or anti-Dyrk1A antibodies (*B*) and then subjected to immunoblot analysis with the indicated antibodies. *C*, co-IP in brain lysates. Mouse brain lysates were immunoprecipitated with control IgG or anti-Dyrk1A antibodies and then subjected to immunoblot analysis with the indicated antibodies. *D*, GST pulldown assay to determine the direct interaction between GSK3β and Dyrk1A. Purified GST or GST-GSK3β fusion protein that was immobilized on beads was incubated with recombinant Dyrk1A protein and subjected to immunoblot analyses.

To identify the specific GSK3β residue that is phosphorylated by Dyrk1A, the amino acid sequences of GSK3β were examined. There were seven potential Dyrk1A-mediated phosphorylation sites (Thr^{43}, Thr^{275}, Thr^{309}, Thr^{324}, Thr^{330}, Thr^{356}, and Ser^{389}) in mouse GSK3β, each of which is followed by a proline residue. Each potential phosphorylation site in GSK3β was changed to alanine, resulting in T43A, T275A, T309A, T324A, T330A, T356A, and S389A. Purified GSK3β K85R and these seven mutants were subjected to kinase assays in the presence of Dyrk1A. The mutation of Thr^{356} to Ala caused a strong decrease in the phosphorylation level of GSK3β, whereas mutations at other positions had little effect on Dyrk1A-dependent phosphorylation (Fig. 2*B*). As shown in Fig. 2*B*, the amounts of GSK3β K85R and mutant proteins used in the kinase assay were similar.

To further confirm the phosphorylation site, three deletion mutants of GSK3β were generated and analyzed by *in vitro* kinase assay. As shown in Fig. 2*C*, the C-terminal domains of GSK3β (343–420) was primarily phosphorylated, whereas the N-terminal domain of GSK3β (1–151) was also weakly phosphorylated, which suggests the existence of other potential phosphorylation sites. Purified GSK3β (343–420) or GSK3β (343–420) (T356A) mutant was then incubated in a kinase buffer that contained [γ-^{32}P]ATP in the presence or absence of Dyrk1A. A band that corresponds to the molecular size of GSK3β (343–420) was detected only in the presence of both GSK3β (343–420) and Dyrk1A (Fig. 2*D*). The Thr^{356} phosphorylation site is located in the C-terminal region of GSK3β and is conserved in humans, rats, and mice. Taken together, these results demonstrate that Dyrk1A selectively phosphorylates Thr^{356} of GSK3β.

Dyrk1A-mediated Phosphorylation of GSK3β inhibits Its Activity—The Thr^{356} phosphorylation site is close to the core of the α-helical domain (152–342) of GSK3β (18). We examined the effect of Dyrk1A-mediated phosphorylation on GSK3β activity. Purified GST-GSK3β bound to glutathione-Sepharose beads was incubated with Dyrk1A in the presence or absence of 10 mM non-radioactive ATP for 1 h at 37 °C, followed by washing the bead-bound GST fusion proteins for the kinase assay using a GSK3 substrate peptide, GSM. The kinase activity of GSK3β that had been phosphorylated by Dyrk1A *in vitro* was reduced by 35 ± 8% ($p < 0.001$) compared with that of non-phosphorylated GSK3β (Fig. 3*A*).

The effect of Dyrk1A-mediated phosphorylation on the activity of GSK3β was further studied using GSK3β WT and the T356A and T356E mutants. The GSK3β phosphorylation-defective S389A mutant, which has been shown previously to activate GSK3β (3), was used as a control. In five independent experiments, the GSK3β T356A and S389A phosphorylation-defective mutants had kinase activity that was enhanced by 65 ± 7% ($p < 0.001$) and 41 ± 8% ($p < 0.01$), respectively, whereas the phosphorylation mimic mutant GSK3β T356E reduced kinase activity by 60 ± 3% ($p < 0.001$) compared with GSK3β WT (Fig. 3*B*). An immunoblot shows that similar amounts of GSK3β WT and the mutant proteins were used for the phosphorylation experiments (Fig. 3*B*). The stimulatory effects of the GSK3β T356A mutant on kinase activity were also confirmed by *in vitro* kinase assays using other known GSK3β substrates, including RCAN1 (Fig. 3*C*) and the C-terminal fragment of amyloid precursor protein (Fig. 3*D*). These results show that *in vitro* Thr^{356} phosphorylation of GSK3β by Dyrk1A inhibits kinase activity.

To confirm the effect of Thr^{356} phosphorylation on GSK3β kinase activity in cells, GSK3β was immunoprecipitated using an anti-Myc antibody from lysates of HEK293T cells that were transfected with plasmids encoding Myc-tagged GSK3β WT or the GSK3β mutants (T356A, T356E, and S389A). In the five independent experiments, the immunoprecipitated GSK3β T356A and S389A mutants enhanced kinase activity by 42 ± 9% ($p < 0.01$) and 42 ± 23% ($p > 0.05$), respectively, whereas the immunoprecipitated GSK3β T356E mutant reduced kinase activity by 66 ± 6% ($p < 0.001$) relative to the GSK3β WT (Fig. 4*A*). The amount of immunoprecipitated GSK3β was similar for GSK3β WT and the mutants (Fig. 4*A*, *bottom panel*). We then examined the effect of GSK3β WT and the mutants on phosphorylation of Tau, which is a well known GSK3β substrate, in HEK293T cells. Western blot analysis was performed with lysates of HEK293T cells that had been transiently transfected with a plasmid expressing Tau either in the presence or absence of a plasmid encoding GSK3β WT or the GSK3β mutants (T356A, T356E, or S389A). Although the amounts of Tau were similar, the Thr(P)^{212}-Tau level was increased in cells that expressed GSK3β T356A and S389A mutants by 26 ± 5% ($p < 0.01$) and 23 ± 4% ($p < 0.01$), respectively, compared with GSK3β WT (Fig. 4*B*). However, the GSK3β T356E mutant showed no significant effect on Tau phosphorylation at Thr^{212} compared with the

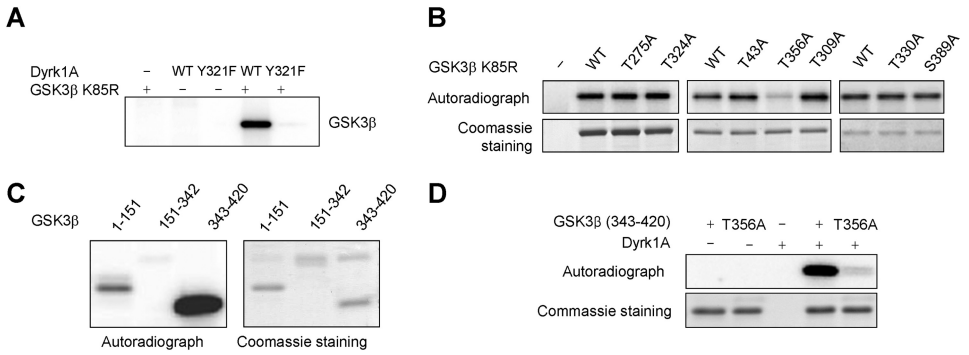

FIGURE 2. **GSK3β is phosphorylated by Dyrk1A at the Thr^{356} residue *in vitro*.** *A*, autoradiograph of SDS-polyacrylamide gels that contained the products of *in vitro* kinase assays with an inactive form of GSK3β (GSK3β K85R) substrate and Dyrk1A WT or the Y321F kinase-inactive mutant. *B*, *top row*, autoradiograph of SDS-polyacrylamide gels that contained the products of the *in vitro* kinase assays that were performed using GSK3β K85R substrates (WT and mutants) and Dyrk1A. *Bottom row*, Coomassie staining of SDS-polyacrylamide gels that contained purified recombinant WT and mutant GSK3β proteins. *C*, *left panel*, autoradiography of SDS-polyacrylamide gels that contained the products of *in vitro* kinase assays that used GSK3β deletion mutant proteins and Dyrk1A. *Right panel*, Coomassie staining of SDS-polyacrylamide gels that contained purified GSK3β deletion mutant proteins. *D*, autoradiography (*top panel*) of SDS-polyacrylamide gels that contained the products of *in vitro* kinase assays that employed purified GSK3β (343–420) or GSK3β (343–420) (T356A) mutants in the presence or absence of Dyrk1A. *Bottom panel*, Coomassie staining of SDS-polyacrylamide gels that contained purified GSK3β mutant proteins.

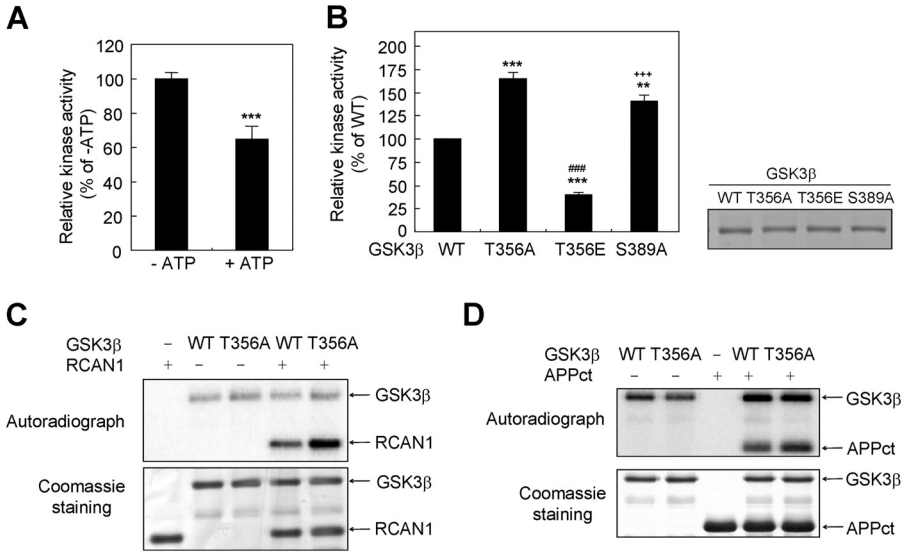

FIGURE 3. **Dyrk1A-mediated phosphorylation of GSK3β at Thr^{356} inhibits its activity *in vitro*.** *A*, purified GST-GSK3β protein that was immobilized on glutathione-Sepharose beads was incubated with Dyrk1A in the presence or absence of ATP. The bead-bound GST fusion proteins were washed and subjected to kinase assays with a GSK3 substrate peptide, GSM. ***, $p < 0.001$ *versus* ATP by Student's *t* test. *B*, purified GST-GSK3β proteins, either WT or mutant forms (T356A, T356E, or S389A) were subjected to kinase assays with a GSM substrate peptide. Coomassie staining of SDS-polyacrylamide gels that contained purified recombinant WT and mutant GSK3β proteins are shown on the right. **, $p < 0.01$; ***, $p < 0.001$ *versus* GSK3β WT; ###, $p < 0.001$ *versus* GSK3β T356A; +++, $p < 0.001$ *versus* GSK3β T356E in analysis of variance followed by Bonferroni post hoc test. *C* and *D*, autoradiographs (*top panels*) and Coomassie staining (*bottom panels*) of SDS-polyacrylamide gels containing the products of *in vitro* kinase assays that used purified RCAN1 proteins (*C*) or C-terminal fragment of amyloid precursor protein (*APPct*, *D*) in the presence or absence of GSK3β (WT or T356A mutant).

cells that were transfected with GSK3β WT (Fig. 4*B*). The inability of GSK3β T356E to inhibit Tau phosphorylation may be due to the abundant presence of endogenous Tau Thr^{212}-phosphorylating kinases, such as GSK3β and Dyrk1A in HEK293T cells (12, 19).

GSK3β inhibits the transcriptional activity of NFAT through phosphorylation-dependent nuclear export of NFATc (20, 21). The effect of Thr^{356} phosphorylation on NFAT transcriptional activity was examined using GSK3β WT and mutants. In HEK293T cells, GSK3β showed a dose-dependent inhibition in NFAT transcriptional activity (Fig. 4*C*). When 200 ng of GSK3β WT was used in the assay, GSK3β WT inhibited NFAT transcriptional activity by 36%, whereas the GSK3β T356A and S389A mutants reduced NFAT-dependent transcription by 44 and 48%, respectively (Fig. 4*D*). In four independent experiments, the GSK3β T356A and S389A mutants showed 10 ± 1% ($p < 0.001$) and 13 ± 3% ($p < 0.05$) reductions, respectively, with regard to the ability of NFAT to inhibit transcription compared with GSK3β WT (Fig. 4*E*). These results indicate that GSK3β inhibition on NFAT transcriptional activity is regulated by phosphorylation of GSK3β at the Thr^{356} and Ser^{389} residues. Taken together, these results support the importance of Thr^{356} phosphorylation for inactivation of GSK3β.

Dyrk1A TG Mice Are Lean and Resistant to Diet-induced Obesity—Dyrk1A can act as a priming kinase for subsequent GSK3β-mediated phosphorylation (16, 22, 23), suggesting additional and/or synergistic roles of Dyrk1A and GSK3β. Our finding that GSK3β is inactivated by Dyrk1A-mediated phosphorylation prompted us to investigate the opposite functional roles of Dyrk1A and GSK3β in cellular processes.

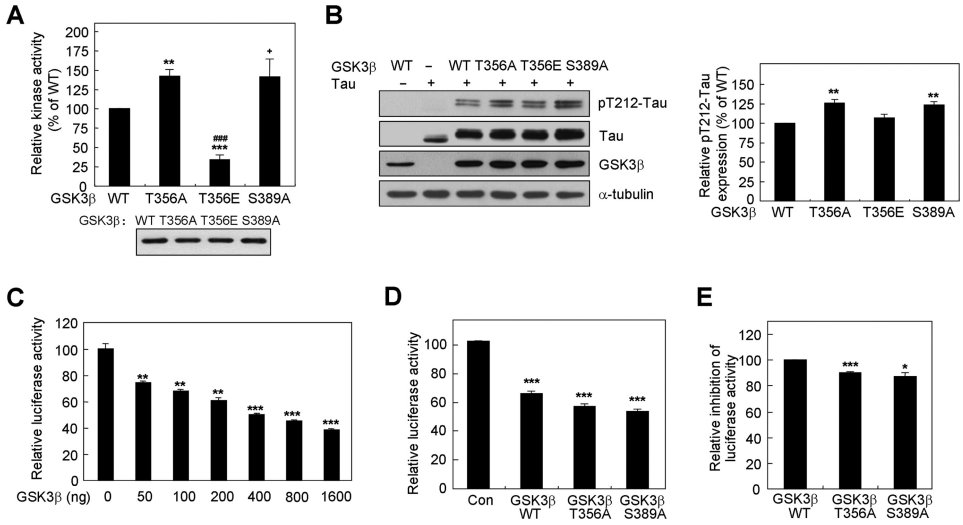

FIGURE 4. **Dyrk1A-mediated phosphorylation of GSK3β at Thr^{356} inhibits its activity in cells.** *A*, GSK3β, immunoprecipitated using an anti-Myc antibody from lysates of HEK293T cells that were transfected with plasmids that encode Myc-tagged GSK3β WT or mutants were subjected to kinase assays. The immunoblot shown below depicts immunoprecipitated GSK3β WT and mutants. **, $p < 0.01$; ***, $p < 0.001$ *versus* GSK3β WT, ###, $p < 0.001$ *versus* GSK3β T356A; +, $p < 0.05$ *versus* GSK3β T356E. *B*, the lysates of HEK293T cells that were transiently transfected with a Tau expression plasmid either in the presence or in the absence of a plasmid encoding GSK3β WT or indicated mutants were subjected to immunoblotting with the indicated antibodies. The results shown in the *left panel* are representative immunoblots. The densitometric analysis of the immunoblots is shown in the *right panel*. **, $p < 0.01$ *versus* GSK3β WT. *C*, HEK293T cells were transfected in triplicate with an NFAT-luciferase reporter construct and the indicated amount of GSK3β. Cells were treated with ionomycin for 48 h and analyzed for reporter gene activity. Luciferase activity was plotted as the percentage of the group without GSK3β. **, $p < 0.01$; ***, $p < 0.001$ *versus* GSK3β (0 ng). *D*, representative experiments measuring NFAT-luciferase transcriptional activity of GSK3β and mutants were performed in quadruplicate. 200 ng of GSK3β WT and the mutants was used for the assay. Luciferase activity was plotted as the percentage of activity compared with the control. ***, $p < 0.001$ *versus* control (*Con*). *E*, inhibition of luciferase activity by GSK3β mutants is plotted as the percent of activity compared with GSK3β WT. *, $p < 0.05$; ***, $p < 0.001$ *versus* GSK3β WT. All data are represented as mean ± S.E. and were analyzed by analysis of variance followed by Bonferroni post hoc test.

It has been reported previously that GSK3β TG mice showed body weight gain that was due to an increased amount of fat (14). Using Dyrk1A TG mice that overexpress Dyrk1A as described previously (9), we first measured the body weight of Dyrk1A TG and control male mice that were placed on a normal chow diet or a 45% HFD over a period of 13 weeks from 5 weeks of age. At around 14 weeks of age, Dyrk1A TG mice on the chow diet showed reduced body weight compared with WT mice. At 18 weeks of age, the body weight of Dyrk1A TG mice was 26.77 ± 0.65 g and that of control mice was 30.56 ± 1.11 g (Fig. 5*A*, $p < 0.05$). The statistically significant body weight difference was more apparent when mice were fed a 45% HFD. Only 5 weeks after HFD treatment, Dyrk1A TG mice clearly started to show resistance to obesity. At week 18, the body weight of Dyrk1A TG mice was 23% lighter than that of WT mice (Fig. 5*B*, Dyrk1A TG, 35.61 ± 1.20 g *versus* control, 46.13 ± 0.67 g, $p < 0.001$). These results indicate that Dyrk1A TG mice are lean and resistant to diet-induced obesity. The average weekly food intake of mice fed a chow diet (Fig. 5*A*) or a 45% HFD (Fig. 5*B*) over a period of 13 weeks from 5 weeks of age was then examined. Consistent with previous observations (24), food consumption was 17% higher in Dyrk1A TG mice fed a chow diet and 23% higher in Dyrk1A TG mice fed a HFD than in controls when food intake was normalized to body weight (Fig. 5*C*). The finding that Dyrk1A TG mice developed a lean phenotype despite their increased food intake prompted us to measure the energy expenditure of mice fed a 45% HFD for 15 weeks. The energy expenditure of Dyrk1A TG mice was 31% higher than that of controls (Fig. 5*D*). Therefore, maintenance of the lean phenotype, regardless of increased food consumption, appears to be attributable to higher metabolic activity in Dyrk1A transgenic mice.

To determine the cause of reduced body weight in Dyrk1A TG mice, we examined fat content. Compared with control mice, visceral epididymal fat pads and perirenal fat pads (with kidney weight) were lower by 60% and by 30%, respectively, in 7-month-old Dyrk1A TG mice fed a chow diet (Fig. 5*E*) when fat weight was normalized by body weight. In Dyrk1A TG mice fed a HFD for 10 weeks, epididymal fat pads and perirenal fat pads (with kidney weight) were lower by 48% and by 30%, respectively, compared with controls when fat weight was normalized by body weight (Fig. 5*F*).

The decreased fat content of Dyrk1A TG mice was further confirmed by MRI to assess adiposity *in vivo*. Cross-sectional images showed that Dyrk1A TG mice had less subcutaneous and visceral fat content of adiposity in mice of various ages (3∼7 months old, Fig. 5*G*). Anatomical views of mice showed reduced fat mass in Dyrk1A TG mice and no difference in body length between Dyrk1A TG and control mice (Dyrk1A TG, 15.5 ± 0.2 cm *versus* control, 15.7 ± 0.4 cm; Fig. 5*H*). Histological analysis of epididymal fat pad sections by staining with H&E showed that the size of adipocytes was smaller for Dyrk1A TG mice than for control mice (Fig. 5*I*). The average diameter of WT adipocytes (95.0 ± 1.4 μm) was 40% longer than those of Dyrk1A TG mice (67.9 ± 0.7 μm, $p < 0.0001$). These results suggest that the lower body weight of Dyrk1A TG mice compared with controls is primarily due to the lower body fat mass of mice. Because the effect of Dyrk1A on body weight and fat masses seems to be the opposite of the effect of GSK3β (14, 25), protein expression in adipocytes was analyzed to understand

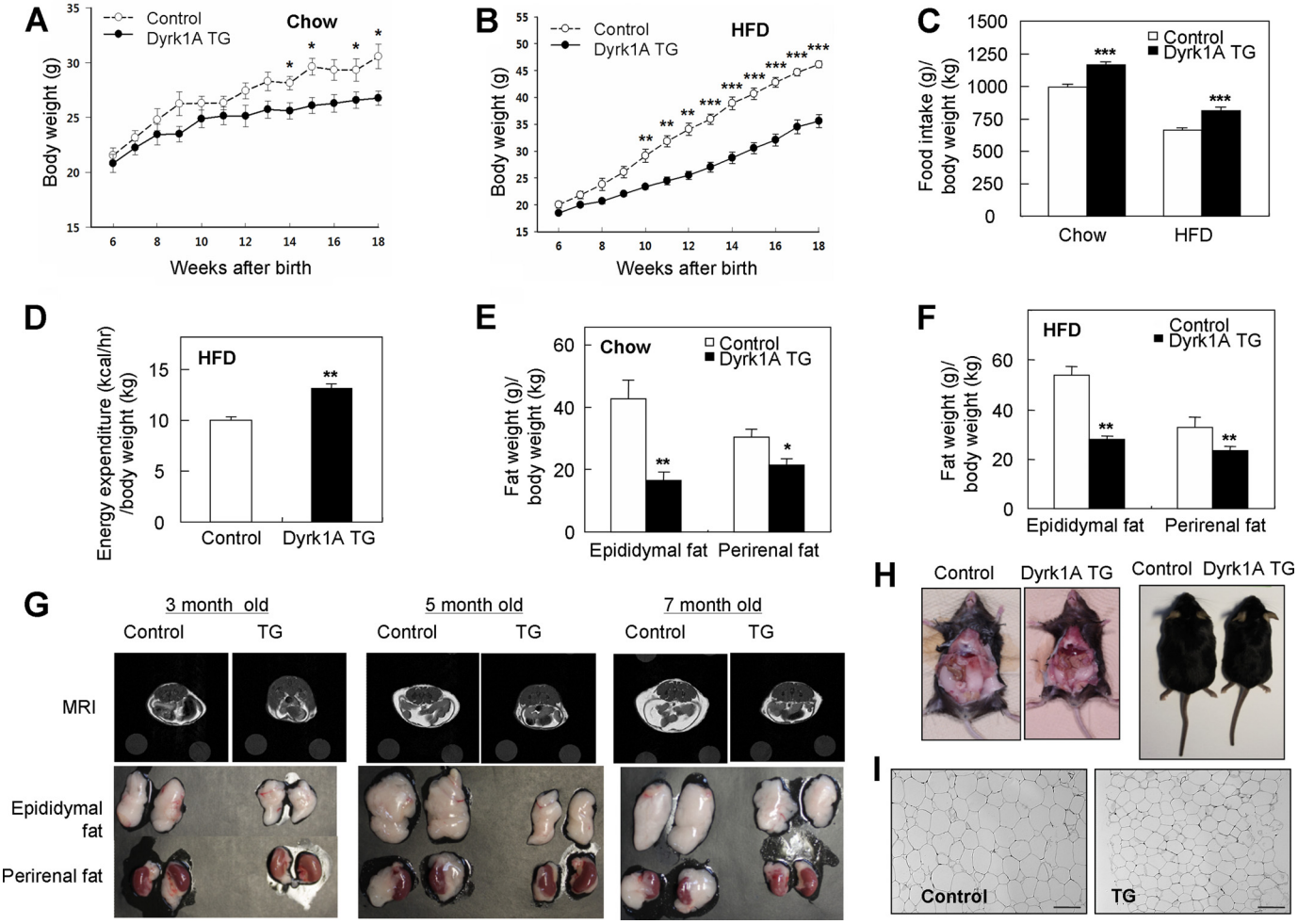

FIGURE 5. **Dyrk1A TG mice are lean and resistant to diet-induced obesity.** *A* and *B*, body weight of Dyrk1A TG (*closed circles*) and control male mice (*open circles*) fed a normal chow diet (*A*) or 45% HFD (*B*). Body weight was measured once per week starting at 5 weeks of age ($n = 4\sim6$). *C*, average weekly food intake per male mouse body weight during weeks 5–18 for mice fed a chow diet or a 45% HFD. *D*, energy expenditure of Dyrk1A TG mice fed a 45% HFD for 15 weeks from week 5 ($n = 5$). *E* and *F*, epididymal and perirenal (with kidney weight) fat content of 7-month-old control and Dyrk1A TG mice that were fed a chow diet (*E*) or of mice that were fed a 45% HFD (*F*) starting at 5 weeks of age and continuing for 10 weeks. The fat weight of each mouse was normalized by its body weight. *G*, representative MRI images of 3- to 7-month-old control and Dyrk1A TG mice that were fed a chow diet. *H*, ventral and dorsal views of 7-month-old control and Dyrk1A TG mice that were fed a chow diet. *I*, reduced adipocyte size of Dyrk1A TG mice. Sections from epididymal fat pads of 7-month-old control and Dyrk1A TG mice were stained with H&E. *Scale bars* = 126 μm. *, $p < 0.05$; **, $p < 0.01$; ***, $p < 0.001$ *versus* control mice by Student's *t* test.

the association between GSK3β and Dyrk1A with regard to the mechanism of obesity.

Thr(P)^{356}-GSK3β Is Expressed in White Adipose Tissue (WAT) and 3T3-L1 Cells—To further investigate the expression of Thr(P)^{356}-GSK3β *in vivo*, a phosphospecific GSK3β antibody was generated. A rabbit polyclonal antibody to the phosphopeptide NGRDT^{356}(PO_4)PALFN was produced and affinity-purified. To test the specificity of the phospho-GSK3β antibody, purified GSK3β was incubated in a kinase buffer in the presence or absence of Dyrk1A (WT or inactive Y321F mutant), and the reaction mixtures were subjected to SDS-PAGE and immunoblotting with phospho-GSK3β antibody. The phospho-GSK3β antibody was only able to detect a band corresponding to GSK3β on the immunoblotted membrane in the presence of both GSK3β and Dyrk1A WT (Fig. 6*A*). To determine whether the Thr(P)^{356}-GSK3β antibody detects GSK3β that phosphorylated at Thr^{356} in cells, Western blot analysis was carried out with lysates of HEK293T cells that had been transiently transfected with GSK3β WT or T356A expression plasmids either alone or in the presence of plasmids encoding Dyrk1A. The Thr(P)^{356}-GSK3β antibody was able to detect a band, but only in the presence of both GSK3β WT and Dyrk1A (Fig. 6*B*), indicating that Dyrk1A phosphorylates GSK3β at Thr^{356}. Furthermore, this phosphorylation does not appear to regulate phosphorylation at the Ser^9 residue (Fig. 6*B*). By immunoblot analysis, the Thr(P)^{356}-GSK3β antibody also revealed a band in GSK3β WT mouse embryonic fibroblast cells but not in the GSK3β$^{-/-}$ mouse embryonic fibroblast cells (Fig. 6*C*), indicating that this antibody detects GSK3β. When mouse WAT lysates were treated with λ-protein phosphatase and Western blotting was performed with the Thr(P)^{356}-GSK3β antibody, the antibody signal disappeared, confirming that the Thr(P)^{356}-GSK3β antibody recognizes the phosphorylated forms of GSK3β (Fig. 6*D*). The specificity of the Thr(P)^{356}-GSK3β antibody was also demonstrated by peptide competition experiments that revealed that the antibody signal in the Western blots of mouse WAT lysates disappeared after preincubation with the GSK3β-phosphopeptide but not with the GSK3β-

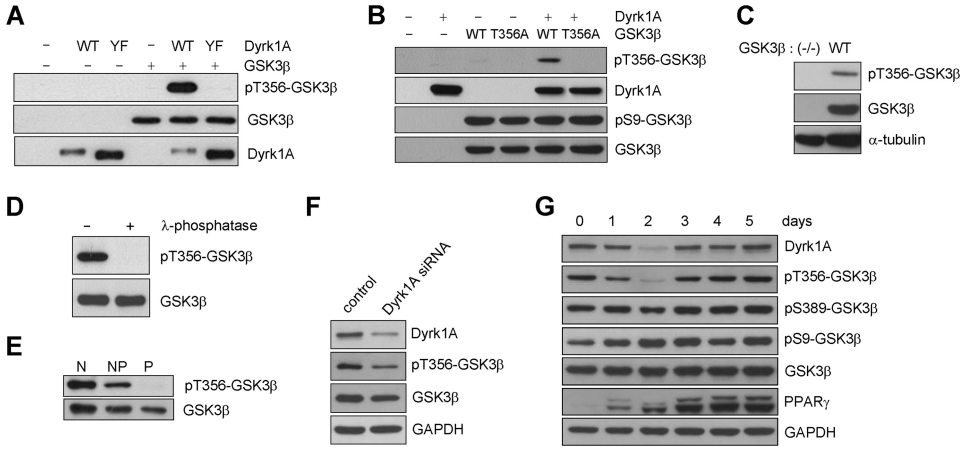

FIGURE 6. **Specificity of Thr(P)^{356}-GSK3β antibody and the expression of Thr(P)^{356}-GSK3β in WAT and 3T3-L1 cells.** *A*, purified GSK3β proteins were subjected to kinase assays in the presence or absence of Dyrk1A (WT or inactive Y321F mutants). The reaction mixtures were subjected to SDS-PAGE and immunoblotting with phospho-GSK3β antibody. *B*, HEK293T cells that were transfected with GSK3β WT or GSK3β T356A expression plasmids in the presence or absence of plasmids encoding Dyrk1A were analyzed by immunoblots with the indicated antibodies. *C*, the lysates of GSK3β WT or GSK3$\beta^{-/-}$ mouse embryonic fibroblast cells were analyzed by immunoblot with the indicated antibodies. *D*, the lysates of WAT were treated with (+) or without (−) λ-protein phosphatase and subsequently analyzed by immunoblot with the Thr(P)^{356}-GSK3β or GSK3β antibodies. E. Peptide competition assay for the pT356-GSK3β antibody. Mouse WAT lysates were analyzed by immunoblot with the Thr(P)^{356}-GSK3β antibody that was preincubated in the absence (*N*) or presence of GSK3β-non-phosphopeptide (*NP*) or GSK3β-phosphopeptide (*P*). *F*, 3T3-L1 cells transfected with Dyrk1A-specific or control siRNA were analyzed by immunoblot with the indicated antibodies. *G*, 2-day post-confluent 3T3-L1 preadipocytes (*day 0*) were induced to differentiate as described under "Experimental Procedures." Differentiated 3T3-L1 cell lysates were analyzed by immunoblot with the indicated antibodies.

non-phosphopeptide (Fig. 6*E*). These results indicate that the phospho-GSK3β antibody was able to specifically identify the phosphorylated GSK3β at Thr^{356}.

To examine whether Dyrk1A phosphorylates GSK3β at Thr^{356} in cells, 3T3-L1 cells were transfected with Dyrk1A-specific or control siRNA. As Dyrk1A siRNA reduced Dyrk1A expression, the level of pT356-GSK3β was also reduced, whereas the expression of GSK3β was similar for the siRNA-transfected cells (Fig. 6*F*). Moreover, to examine the expression of proteins of interest in the adipocyte differentiation process, we analyzed 3T3-L1 cells. After treatment of 3T3-L1 cells with differentiation inducers, the expression of Dyrk1A was reduced for the following 2 days, which corresponds to the mitotic clonal expansion period. Then Dyrk1A expression increased again at day 3, which is the beginning of the maturation phase. The expression of pT356-GSK3β followed a very similar pattern as Dyrk1A expression, whereas Ser(P)^{389}-GSK3β, Ser(P)^{9}-GSK3β, and GSK3β were steadily expressed during differentiation (Fig. 6*G*). Together, these results suggest that Dyrk1A is a kinase that is responsible for phosphorylating GSK3β at Thr^{356}.

Thr(P)^{356}-GSK3β Is Increased in the WAT of Dyrk1A TG Mice—To determine whether the expression of phospho-GSK3β increases in Dyrk1A TG mice, immunoblot analyses were performed with WAT lysates that were prepared from 5- to 9-month-old Dyrk1A TG and control mice fed a chow diet (Fig. 7, *A* and *B*). The level of pT356-GSK3β (normalized by GAPDH) in Dyrk1A TG mice was increased by 74 ± 20% ($p < 0.01$) relative to that of the controls. After normalization to the levels of total GSK3β, the amount of Thr(P)^{356}-GSK3β in Dyrk1A TG mice was increased by 97 ± 31% ($p < 0.05$) compared with the controls. In contrast, the levels of Ser(P)^{9}-GSK3β, Ser(P)^{389}-GSK3β (either normalized by GAPDH or GSK3β), and GSK3β (normalized by GAPDH) did not significantly differ between Dyrk1A TG and control mice (Fig. 7, *A* and *B*), suggesting that Thr(P)^{356}-GSK3β level is specifically increased in the WAT of Dyrk1A TG mice.

To assess the effects of Thr(P)^{356}-GSK3β on the abundance of GS and β-catenin, two well known downstream targets of GSK3β, WAT lysates were analyzed by immunoblotting in Dyrk1A TG and control mice that were fed a chow diet. The level of GS (normalized by GAPDH) increased by 27 ± 7% ($p < 0.05$) in the WAT of Dyrk1A TG mice relative to that of the controls, although cellular β-catenin levels were not altered (Fig. 7, *A* and *B*), suggesting a specific link between Thr(P)^{356}-GSK3β and GS in these mice. Together, these results show that the levels of Thr(P)^{356}-GSK3β increase when Dyrk1A levels increase, revealing the *in vivo* importance of this phosphorylation. The specific increase in the Thr(P)^{356}-GSK3β and GS levels in WAT of Dyrk1A TG mice implies their potential link to the lean phenotype of Dyrk1A TG mice that were fed a chow diet (Fig. 5*A*).

We then determined the expression of phospho-GSK3β in WAT lysates prepared from 5- to 9-month-old Dyrk1A TG and control mice fed a HFD (Fig. 8, *A* and *B*). The amount of Thr(P)^{356}-GSK3β in the Dyrk1A TG mice was increased by 63 ± 8% ($p < 0.001$, normalized by GAPDH) and 37 ± 7% ($p < 0.01$, normalized by GSK3β) relative to that of the controls. The levels of Ser(P)^{9}- and Ser(P)^{389}-GSK3β (normalized by GAPDH) also increased by 51 ± 22% ($p < 0.05$) and 94 ± 10% ($p < 0.001$), respectively, relative to the controls. After normalization to the levels of GSK3β, the amount of Ser(P)^{389}-GSK3β in the Dyrk1A TG mice increased by 62 ± 1% ($p < 0.001$) compared with the controls. Furthermore, the levels of GSK3β, GS, and β-catenin (normalized by GAPDH) were also increased by 19 ± 6% ($p < 0.01$), 75 ± 32% ($p < 0.01$), and 74 ± 14% ($p < 0.01$), respectively, relative to the controls (Fig. 8*B*). These results reveal that, under HFD conditions, the levels of inactive phosphorylated forms of GSK3β, Thr(P)^{356}-GSK3β, Ser(P)^{9}-GSK3β, and Ser(P)^{389}-GSK3β, as well as the levels of down-

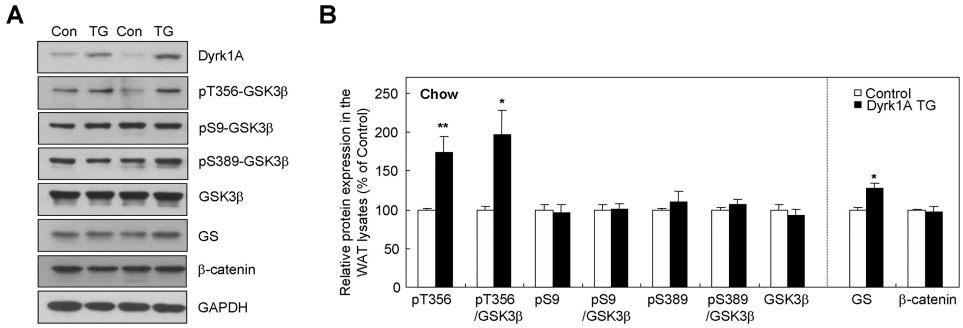

FIGURE 7. **Thr(P)^{356}-GSK3β is increased in the WAT of Dyrk1A TG mice that were fed a normal diet.** Shown are representative immunoblots (*A*) and densitometric analysis (*B*) of WAT lysates of Dyrk1A TG mice and control (*Con*) mice fed a normal chow ($n = 4\sim6$). WAT lysates of mice at 5–9 months of age were used for analysis. The phospho-GSK3β signals in the immunoblots were normalized by GAPDH and GSK3β signals. The GSK3β, GS, and β-catenin signals were normalized by GAPDH. *, $p < 0.05$; **, $p < 0.01$ *versus* control mice by Student's *t* test.

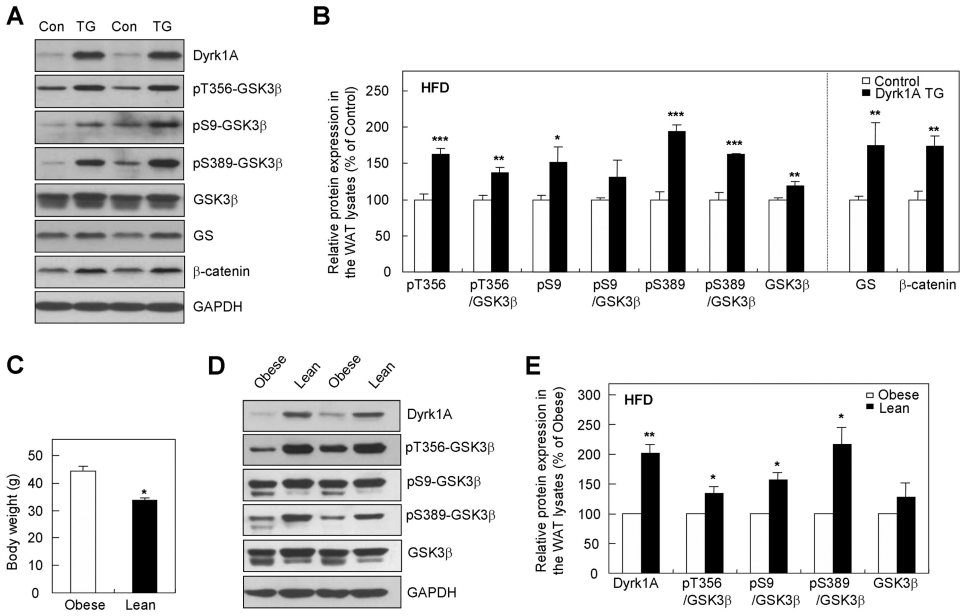

FIGURE 8. **Thr(P)^{356}-GSK3β is increased in the WAT of Dyrk1A TG mice that were fed a HFD.** *A* and *B*, representative immunoblots (*A*) and densitometric analysis (*B*) of WAT lysates of 5–9 month-old Dyrk1A TG and control (*Con*) mice fed a HFD ($n = 6\sim10$). The amounts of phospho-GSK3β, GS, and β-catenin of Dyrk1A TG are plotted as a percentage compared with control mice. *, $p < 0.05$; **, $p < 0.01$; ***, $p < 0.001$ *versus* control mice by Student's *t* test. *C*, body weight of obese and lean control littermates fed an HFD. *, $p < 0.05$ *versus* obese mice by Student's *t* test. *D* and *E*, representative immunoblots (*D*) and densitometric analysis (*E*) of WAT lysates of obese and lean mice that were fed a HFD ($n = 5$). WAT lysates of mice at 5–9 months of age were used for analysis. The amounts of phospho-GSK3β, GS, and β-catenin of lean mice are plotted as a percentage compared with obese mice. Data are represented as means ± S.E. *, $p < 0.05$; **, $p < 0.01$ *versus* obese mice by Student's *t* test.

stream targets of GSK3β, GS, and β-catenin, are all enhanced when Dyrk1A is overexpressed. These results show a connection between inactivity of GSK3β and GS/β-catenin abundance in WAT of Dyrk1A TG mice, which may be responsible for the lean phenotype of Dyrk1A TG mice that were fed a HFD (Fig. 5*B*).

Additionally, we unexpectedly observed different propensities to HFD-induced obesity among control littermates with regard to body weight. Consistent with previous reports of humans and rodents (26), some mice became obese and others became lean. The body weight of lean mice used in analyses was 23% less than that of their obese littermates at week 18 (Fig. 8*C*). Immunoblotting analysis was performed with WAT lysates of lean and obese littermate mice that were fed a HFD. In WAT, Dyrk1A expression (normalized by GAPDH) in the lean mice was increased by 102 ± 14% ($p < 0.01$) compared with the obese mice. Accordingly, the amounts of Thr(P)^{356}-GSK3β, Ser(P)^{9}-GSK3β, and Ser(P)^{389}-GSK3β, after normalization to the levels of total GSK3β, in the lean mouse WAT, increased by 34 ± 11% ($p < 0.05$), 56 ± 14% ($p < 0.05$), and 116 ± 29% ($p < 0.05$), respectively, relative to the obese littermates (Fig. 8, *D* and *E*). In contrast, the levels of GSK3β (normalized by GAPDH) did not significantly differ between lean and obese mice, although a trend toward a high GSK3β level was observed (Fig. 8, *D* and *E*). These results, together with the lean phenotype of Dyrk1A TG mice (Fig. 5), support the idea that Dyrk1A overexpression may lead to an obesity-resistant phenotype.

Expression of Adipogenic Proteins Is Decreased in 3T3-L1 Cells Overexpressing Dyrk1A and in the WAT of Young Dyrk1A TG Mice Fed a Chow Diet—Because adipogenesis is a potential mechanism leading to the obesity-resistant phenotype in Dyrk1A TG mice, we determined the effect of Dyrk1A overexpression on preadipocyte differentiation and the expression of adipogenesis marker proteins in 3T3-L1 cells. To assess accu-

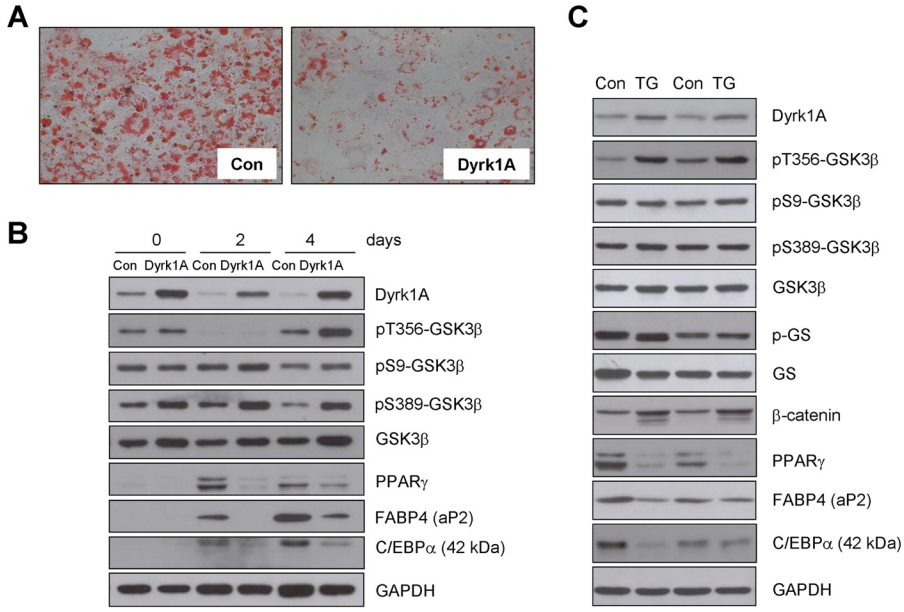

FIGURE 9. **Effect of Dyrk1A overexpression on preadipocyte differentiation and expression of adipogenesis marker proteins.** *A*, 3T3-L1 cells overexpressing Dyrk1A and control (*Con*) cells were differentiated for 8 days and then fixed and stained with Oil Red O. *B*, 3T3-L1 cells overexpressing Dyrk1A and control cells were differentiated for the indicated number of days and analyzed by Western blot to characterize protein expression. *C*, representative immunoblots of WAT lysates of 8-week-old Dyrk1A TG and control mice fed a normal chow diet.

mulation of lipid droplets, 3T3-L1 cells were transfected with control or Dyrk1A cDNA plasmids and selected in the presence of G418, followed by differentiation and Oil Red O staining. As demonstrated by a reduction in the number of Oil Red O-positive cells, adipocyte differentiation was strongly inhibited in cells overexpressing Dyrk1A (Fig. 9*A*). 3T3-L1 cells overexpressing Dyrk1A were also generated by infection with Dyrk1A lentiviral stocks produced from HEK293 cells. Blasticidin-selected 3T3-L1 cells were differentiated, and protein expression was analyzed by Western blotting. Compared with control 3T3-L1 cells, overexpression of Dyrk1A increased the level of Thr(P)^{356}-GSK3β in addition to the levels of Ser(P)^{9}-GSK3β, Ser(P)^{389}-GSK3β and GSK3β. Furthermore, overexpression of Dyrk1A inhibited the expression of key adipogenesis regulators, including PPARγ and C/EBPα, and a PPARγ target, FABP4 (Fig. 9*B*).

Elevated Thr(P)^{356}-GSK3β levels were observed in Dyrk1A TG mice and lean mice from the control group at 5–9 months of age (Figs. 7 and Fig. 8). To determine the effect of Dyrk1A overexpression on the expression of adipogenic proteins in younger mice, immunoblot analyses were performed with WAT lysates prepared from 8-week-old Dyrk1A TG and control mice fed a chow diet (Fig. 9*C*). The level of Thr(P)^{356}-GSK3β, but not the levels of Ser(P)^{9}-GSK3β, Ser(P)^{389}-GSK3β, or GSK3β, was higher in Dyrk1A TG mice than in controls. Concordant with the decreased PPARγ expression observed in 3T3-L1 cells overexpressing Dyrk1A, the expression of major adipogenic transcription factors, such as PPARγ and C/EBPα, was lower in Dyrk1A TG mice than in controls. The level of FABP4 (aP2) was also reduced in Dyrk1A TG mice. In contrast to the results observed for 5- to 9-month-old Dyrk1A TG mice fed a chow diet (Fig. 7, *A* and *B*), the level of β-catenin, but not of GS, was increased in the WAT of 8-week-old Dyrk1A TG mice (Fig. 9*C*). Collectively, these results suggest a specific link among Thr(P)^{356}-GSK3β, β-catenin, and key adipogenic transcription factors in young Dyrk1A TG mice fed a chow diet.

DISCUSSION

In this study, we showed, for the first time, that Dyrk1A interacts with and phosphorylates GSK3β at the Thr^{356} residue and that this phosphorylation inhibits GSK3β activity. We found that Dyrk1A TG mice are lean and resistant to diet-induced obesity, which shows an inverse correlation to the effect of GSK3β on obesity. The levels of Thr(P)^{356}-GSK3β were increased in the WAT of Dyrk1A TG mice, providing *in vivo* evidence of GSK3β phosphorylation by Dyrk1A. Furthermore, enhanced levels of Thr(P)^{356}-GSK3β in Dyrk1A TG mice fed a chow diet led to differential regulation of β-catenin and GS, key downstream targets of GSK3β, depending on the age of the mice. These results reveal a novel regulatory connection between Dyrk1A and GSK3β with regard to the mechanism of obesity.

GSK3β is active in unstimulated cells and primarily regulated by the phosphorylation of specific residues and subsequent inactivation. Inhibition of GSK3β activity can occur as the result of phosphorylation at the Ser^{9} and Ser^{389} residues (3, 27). Phosphorylation of GSK3β at Ser^{9} by Akt and other kinases is a major mechanism by which GSK3β is inactivated (1, 2). ERK-mediated phosphorylation of GSK3β at the Thr^{43} residue primes GSK3β for subsequent phosphorylation at Ser^{9}, which leads to inactivation of GSK3β (28). Phosphorylation at Ser^{389} or Thr^{390} of the mouse or human GSK3β by p38 MAPK also inactivates GSK3β, resulting in an increased amount of β-catenin (3). However, the regulatory mechanism of GSK3β is more diverse and not fully understood. Our study shows a new pathway for GSK3β inactivation by phosphorylation at the Thr^{356} residue by Dyrk1A. GSK3β and Dyrk1A appear to play an additional and/or synergistic role in health and in disease.

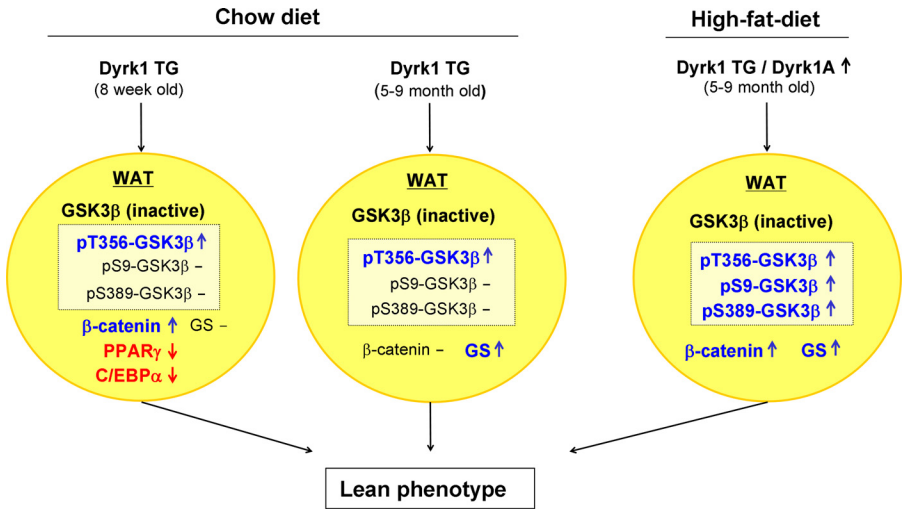

FIGURE 10. **Schematic for the hypothetical role of Dyrk1A in the mechanism of obesity resistance.** ↑, increase; ↓, decrease; –, no change.

Dyrk1A is able to act as a priming kinase for subsequent GSK3β-mediated phosphorylation (16, 22, 23). Both GSK3β and Dyrk1A are implicated in the pathogenesis of AD. Considering the critical role of GSK3β in numerous fundamental cellular processes and in a variety of human diseases such as obesity, type 2 diabetes, cancer, and AD, it is important to fully understand the regulatory mechanism of GSK3β activity for the development of potential treatment of these diseases. Although further research on the role of Dyrk1A-mediated GSK3β inactivation in a variety of GSK3β function still needs to be conducted, this study focused on obesity because of the apparent opposite effect of Dyrk1A and GSK3β on body weight and fat content.

GSK3 activity specifically increased in the adipose tissue of obese mice, and the GSK3 inhibitor prevents adipocyte differentiation (29, 30), which supports a connection between increased GSK3 activity and obesity. Simultaneous knockdown of GSK3α and GSK3β showed a strong decrease in body weight (31), whereas GSK3β TG mice that overexpress human GSK3β in skeletal muscle showed body weight gain that was due to an increased amount of fat (14). Moreover, a small-molecule GSK3 inhibitor shows anti-obesity effects on HFD-induced obesity as a result of decreased adiposity and improved lipid profiles (25). GSK3β plays an important role in adipogenesis through the Wnt/β-catenin-dependent pathway (30, 32). Wnt signaling blocks preadipocyte differentiation through inhibition of the adipogenic transcription factors C/EBPα and PPARγ (32). Our results in 8-week-old Dyrk1A TG mice fed a chow diet (Fig. 9*C*) support attribution of the anti-adipogenic effect of Dyrk1A to the up-regulation of β-catenin through inactivation and phosphorylation at Thr^{356} of GSK3β, resulting in inhibition of expression of PPARγ and C/EBPα (Fig. 10). GSK3β is also a negative regulator of GS, which is the most commonly studied GSK3β *in vivo* substrate. Constitutive activation of GSK3β down-regulates GS protein abundance, which results in reduced glycogenesis, whereas small molecule GSK3β inhibitors elevate GS protein level (33). We observed diet-dependent differential regulation of GSK3β activity by phosphorylation at different sites in the adipose tissue of mice at 5–9 months of age. Under chow diet conditions, the level of $Thr(P)^{356}$-GSK3β, but not of $Ser(P)^{9}$-GSK3β and $Ser(P)^{389}$-GSK3β, was specifically increased in the WAT of Dyrk1A TG mice, resulting in a specific increase in the level of GS without alteration in β-catenin level (Fig. 7, *A* and *B*). In contrast, under HFD conditions, levels of inactive phosphorylated forms, including $Thr(P)^{356}$-GSK3β, $Ser(P)^{9}$-GSK3β, and $Ser(P)^{389}$-GSK3β, were increased, generating increased levels of GSK3β downstream targets, GS, and β-catenin, in the WAT of Dyrk1A TG mice compared with control mice (Fig. 8, *A* and *B*). These results suggest that, at 5–9 months of age, GS abundance is possibly caused by increased phosphorylation of GSK3β at Thr^{356} in Dyrk1A TG mice that were fed a chow diet, whereas increased GS and β-catenin levels are caused by elevated $Ser(P)^{9}$-GSK3β, $Ser(P)^{389}$-GSK3β, and $Thr(P)^{356}$-GSK3β in Dyrk1A TG mice that were fed a HFD. Although a direct link between GS level and obesity is not well understood, these results support an association between Dyrk1A overexpression, GSK3β inactivity, and an obesity-resistant phenotype. Therefore, increased $Thr(P)^{356}$-GSK3β expression in Dyrk1A TG mice may cause differential regulation of β-catenin and GS, depending on the age and the diet of the mice (Fig. 10).

In addition to the multiple biological functions of Dyrk1A through phosphorylation of diverse proteins (6), this study reveals a new role of Dyrk1A in obesity. Increased expression of Dyrk1A in Dyrk1A TG or lean mice shows resistance to HFD-induced obesity (Figs. 5 and 8). In Dyrk1A TG mice, the lower body weight is primarily due to lower body fat content (Fig. 5). Consistent with our results, Dyrk1A-haploinsufficient ($Dyrk1A^{+/-}$) mice were heavier than controls (34), mostly because of increased abdominal fat. Inverse effects of Dyrk1A and GSK3β on body weight and fat content support the role of Dyrk1A-mediated GSK3β inactivation in obesity. Further investigations that examine the expression of Dyrk1A and $Thr(P)^{356}$-GSK3β in lean and obese humans and in animal adipocytes and/or analyze GSK3β T356A knockin mutant will be necessary to substantiate the functional importance of this phosphorylation event in obesity.

Although phosphorylation and inactivation of GSK3β by Dyrk1A, at least in part, explain the mechanism of obesity resistance, alternative explanations may exist regarding the role

of Dyrk1A in obesity resistance, considering the multifunctional nature of Dyrk1A. It has been reported that TG mice that overexpress Sirt1, which is an NAD-dependent protein deacetylase that is implicated in energy metabolism, are leaner and metabolically more active, whereas the Sirt1 activator resveratrol can protect against diet-induced obesity and insulin resistance (35). Dyrk1A phosphorylates Sirt1, which results in increased Sirt1 deacetylase activity (36). Therefore, overexpression of Dyrk1A may contribute to the lean phenotype through phosphorylation and activation of Sirt1. Moreover, reports that overexpression of Dyrk1A decreases endogenous NFAT levels (21) and that NFAT knockout mice have defects in fat accumulation and are protected from diet-induced obesity (37) also support the potential role of Dyrk1A in obesity through the NFAT-dependent pathway.

On the basis of our results, we propose the following mechanism for the regulation of GSK3β activity in obesity. Overexpression of Dyrk1A inhibits GSK3β activity through phosphorylation at the Thr^{356} residue, and this process may contribute to the obesity-resistant phenotype, especially under normal chow diet conditions. Although the exact role of Dyrk1A in obesity requires further investigation, the obesity-resistant phenotype in Dyrk1A TG mice might be, at least in part, mediated by GSK3β inactivation. Our findings reveal a novel regulatory mechanism for GSK3β activity and provide insight into the mechanism of obesity, proposing that Dyrk1A and $Thr(P)^{356}$-GSK3β may serve as potential therapeutic targets for the development of drugs to treat obesity.

Acknowledgments—We thank Dr. Jae-woo Kim (Yonsei University) for helpful suggestions and Dr. Cheol Soo Choi (Gachon University) for energy expenditure data. We also thank So Young Park, Jung-Yeon Kwon, and Hye Jin Yun for technical support.

REFERENCES

1. Stambolic, V., and Woodgett, J. R. (1994) Mitogen inactivation of glycogen synthase kinase-3 β in intact cells via serine 9 phosphorylation. *Biochem. J.* **303,** 701–704
2. Jope, R. S., and Johnson, G. V. (2004) The glamour and gloom of glycogen synthase kinase-3. *Trends Biochem. Sci* **29,** 95–102
3. Thornton, T. M., Pedraza-Alva, G., Deng, B., Wood, C. D., Aronshtam, A., Clements, J. L., Sabio, G., Davis, R. J., Matthews, D. E., Doble, B., and Rincon, M. (2008) Phosphorylation by p38 MAPK as an alternative pathway for GSK3β inactivation. *Science* **320,** 667–670
4. Frame, S., and Cohen, P. (2001) GSK3 takes centre stage more than 20 years after its discovery. *Biochem. J.* **359,** 1–16
5. Doble, B. W., and Woodgett, J. R. (2003) GSK-3: tricks of the trade for a multi-tasking kinase. *J. Cell Sci.* **116,** 1175–1186
6. Park, J., Song, W. J., and Chung, K. C. (2009) Function and regulation of Dyrk1A: towards understanding Down syndrome. *Cell. Mol. Life Sci.* **66,** 3235–3240
7. Fotaki, V., Dierssen, M., Alcántara, S., Martínez, S., Martí, E., Casas, C., Visa, J., Soriano, E., Estivill, X., and Arbonés, M. L. (2002) Dyrk1A haploinsufficiency affects viability and causes developmental delay and abnormal brain morphology in mice. *Mol. Cell. Biol.* **22,** 6636–6647
8. Smith, D. J., Stevens, M. E., Sudanagunta, S. P., Bronson, R. T., Makhinson, M., Watabe, A. M., O'Dell, T. J., Fung, J., Weier, H. U., Cheng, J. F., and Rubin, E. M. (1997) Functional screening of 2 Mb of human chromosome 21q22.2 in transgenic mice implicates minibrain in learning defects associated with Down syndrome. *Nat. Genet.* **16,** 28–36
9. Ahn, K. J., Jeong, H. K., Choi, H. S., Ryoo, S. R., Kim, Y. J., Goo, J. S., Choi, S. Y., Han, J. S., Ha, I., and Song, W. J. (2006) DYRK1A BAC transgenic mice show altered synaptic plasticity with learning and memory defects. *Neurobiol. Dis.* **22,** 463–472
10. Kimura, R., Kamino, K., Yamamoto, M., Nuripa, A., Kida, T., Kazui, H., Hashimoto, R., Tanaka, T., Kudo, T., Yamagata, H., Tabara, Y., Miki, T., Akatsu, H., Kosaka, K., Funakoshi, E., Nishitomi, K., Sakaguchi, G., Kato, A., Hattori, H., Uema, T., and Takeda, M. (2007) The DYRK1A gene, encoded in chromosome 21 Down syndrome critical region, bridges between β-amyloid production and Tau phosphorylation in Alzheimer disease. *Hum. Mol. Genet.* **16,** 15–23
11. Ryoo, S. R., Cho, H. J., Lee, H. W., Jeong, H. K., Radnaabazar, C., Kim, Y. S., Kim, M. J., Son, M. Y., Seo, H., Chung, S. H., and Song, W. J. (2008) Dual-specificity tyrosine(Y)-phosphorylation regulated kinase 1A-mediated phosphorylation of amyloid precursor protein: evidence for a functional link between Down syndrome and Alzheimer's disease. *J. Neurochem.* **104,** 1333–1344
12. Ryoo, S. R., Jeong, H. K., Radnaabazar, C., Yoo, J. J., Cho, H. J., Lee, H. W., Kim, I. S., Cheon, Y. H., Ahn, Y. S., Chung, S. H., and Song, W. J. (2007) DYRK1A-mediated hyperphosphorylation of Tau: a functional link between Down syndrome and Alzheimer disease. *J. Biol. Chem.* **282,** 34850–34857
13. Ryu, Y. S., Park, S. Y., Jung, M. S., Yoon, S. H., Kwen, M. Y., Lee, S. Y., Choi, S. H., Radnaabazar, C., Kim, M. K., Kim, H., Kim, K., Song, W. J., and Chung, S. H. (2010) Dyrk1A-mediated phosphorylation of Presenilin 1: a functional link between Down syndrome and Alzheimer's disease. *J. Neurochem.* **115,** 574–584
14. Pearce, N. J., Arch, J. R., Clapham, J. C., Coghlan, M. P., Corcoran, S. L., Lister, C. A., Llano, A., Moore, G. B., Murphy, G. J., Smith, S. A., Taylor, C. M., Yates, J. W., Morrison, A. D., Harper, A. J., Roxbee-Cox, L., Abuin, A., Wargent, E., and Holder, J. C. (2004) Development of glucose intolerance in male transgenic mice overexpressing human glycogen synthase kinase-3β on a muscle-specific promoter. *Metabolism* **53,** 1322–1330
15. Park, J. H., Jung, M. S., Kim, Y. S., Song, W. J., and Chung, S. H. (2012) Phosphorylation of Munc18–1 by Dyrk1A regulates its interaction with Syntaxin 1 and X11α. *J. Neurochem.* **122,** 1081–1091
16. Jung, M. S., Park, J. H., Ryu, Y. S., Choi, S. H., Yoon, S. H., Kwen, M. Y., Oh, J. Y., Song, W. J., and Chung, S. H. (2011) Regulation of RCAN1 protein activity by Dyrk1A protein-mediated phosphorylation. *J. Biol. Chem.* **286,** 40401–40412
17. Lee, H., Lee, Y. J., Choi, H., Ko, E. H., and Kim, J. W. (2009) Reactive oxygen species facilitate adipocyte differentiation by accelerating mitotic clonal expansion. *J. Biol. Chem.* **284,** 10601–10609
18. Dajani, R., Fraser, E., Roe, S. M., Young, N., Good, V., Dale, T. C., and Pearl, L. H. (2001) Crystal structure of glycogen synthase kinase 3β: structural basis for phosphate-primed substrate specificity and autoinhibition. *Cell* **105,** 721–732
19. Zheng-Fischhöfer, Q., Biernat, J., Mandelkow, E. M., Illenberger, S., Godemann, R., and Mandelkow, E. (1998) Sequential phosphorylation of Tau by glycogen synthase kinase-3β and protein kinase A at Thr212 and Ser214 generates the Alzheimer-specific epitope of antibody AT100 and requires a paired-helical-filament-like conformation. *Eur. J. Biochem.* **252,** 542–552
20. Beals, C. R., Sheridan, C. M., Turck, C. W., Gardner, P., and Crabtree, G. R. (1997) Nuclear export of NF-ATc enhanced by glycogen synthase kinase-3. *Science* **275,** 1930–1934
21. Arron, J. R., Winslow, M. M., Polleri, A., Chang, C. P., Wu, H., Gao, X., Neilson, J. R., Chen, L., Heit, J. J., Kim, S. K., Yamasaki, N., Miyakawa, T., Francke, U., Graef, I. A., and Crabtree, G. R. (2006) NFAT dysregulation by increased dosage of DSCR1 and DYRK1A on chromosome 21. *Nature* **441,** 595–600
22. Kurabayashi, N., Hirota, T., Sakai, M., Sanada, K., and Fukada, Y. (2010) DYRK1A and glycogen synthase kinase 3β, a dual-kinase mechanism directing proteasomal degradation of CRY2 for circadian timekeeping. *Mol. Cell. Biol.* **30,** 1757–1768
23. Woods, Y. L., Cohen, P., Becker, W., Jakes, R., Goedert, M., Wang, X., and Proud, C. G. (2001) The kinase DYRK phosphorylates protein-synthesis initiation factor eIF2Bε at Ser539 and the microtubule-associated protein

Tau at Thr212: potential role for DYRK as a glycogen synthase kinase 3-priming kinase. *Biochem. J.* **355,** 609–615
24. Hong, S. H., Lee, K. S., Kwak, S. J., Kim, A. K., Bai, H., Jung, M. S., Kwon, O. Y., Song, W. J., Tatar, M., and Yu, K. (2012) Minibrain/Dyrk1a regulates food intake through the Sir2-FOXO-sNPF/NPY pathway in *Drosophila* and mammals. *PLOS Genet.* **8,** e1002857
25. Lee, S., Yang, W. K., Song, J. H., Ra, Y. M., Jeong, J. H., Choe, W., Kang, I., Kim, S. S., and Ha, J. (2013) Anti-obesity effects of 3-hydroxychromone derivative, a novel small-molecule inhibitor of glycogen synthase kinase-3. *Biochem. Pharmacol.* **85,** 965–976
26. Chang, S., Graham, B., Yakubu, F., Lin, D., Peters, J. C., and Hill, J. O. (1990) Metabolic differences between obesity-prone and obesity-resistant rats. *Am. J. Physiol.* **259,** R1103–R1110
27. Sutherland, C., Leighton, I. A., and Cohen, P. (1993) Inactivation of glycogen synthase kinase-3 β by phosphorylation: new kinase connections in insulin and growth-factor signalling. *Biochem. J.* **296,** 15–19
28. Ding, Q., Xia, W., Liu, J. C., Yang, J. Y., Lee, D. F., Xia, J., Bartholomeusz, G., Li, Y., Pan, Y., Li, Z., Bargou, R. C., Qin, J., Lai, C. C., Tsai, F. J., Tsai, C. H., and Hung, M. C. (2005) Erk associates with and primes GSK-3β for its inactivation resulting in upregulation of β-catenin. *Mol. Cell.* **19,** 159–170
29. Eldar-Finkelman, H., Schreyer, S. A., Shinohara, M. M., LeBoeuf, R. C., and Krebs, E. G. (1999) Increased glycogen synthase kinase-3 activity in diabetes- and obesity-prone C57BL/6J mice. *Diabetes* **48,** 1662–1666
30. Bennett, C. N., Ross, S. E., Longo, K. A., Bajnok, L., Hemati, N., Johnson, K. W., Harrison, S. D., and MacDougald, O. A. (2002) Increased glycogen synthase kinase-3 activity in diabetes- and obesity-prone C57BL/6J mice. *J. Biol. Chem.* **277,** 30998–31004
31. Steuber-Buchberger, P., Wurst, W., and Kühn, R. (2008) Simultaneous Cre-mediated conditional knockdown of two genes in mice. *Genesis* **46,** 144–151
32. Ross, S. E., Hemati, N., Longo, K. A., Bennett, C. N., Lucas, P. C., Erickson, R. L., and MacDougald, O. A. (2000) Inhibition of adipogenesis by Wnt signaling. *Science* **289,** 950–953
33. MacAulay, K., Blair, A. S., Hajduch, E., Terashima, T., Baba, O., Sutherland, C., and Hundal, H. S. (2005) Constitutive activation of GSK3 downregulates glycogen synthase abundance and glycogen deposition in rat skeletal muscle cells. *J. Biol. Chem.* **280,** 9509–9518
34. Rachdi, L., Kariyawasam, D., Guez, F., Aïello, V., Arbonés, M. L., Janel, N., Delabar, J. M., Polak, M., and Scharfmann, R. (2014) Dyrk1a haploinsufficiency induces diabetes in mice through decreased pancreatic β cell mass. *Diabetologia* **57,** 960–969
35. Lagouge, M., Argmann, C., Gerhart-Hines, Z., Meziane, H., Lerin, C., Daussin, F., Messadeq, N., Milne, J., Lambert, P., Elliott, P., Geny, B., Laakso, M., Puigserver, P., and Auwerx, J. (2006) Resveratrol improves mitochondrial function and protects against metabolic disease by activating SIRT1 and PGC-1α. *Cell* **127,** 1109–1122
36. Guo, X., Williams, J. G., Schug, T. T., and Li, X. (2010) DYRK1A and DYRK3 promote cell survival through phosphorylation and activation of SIRT1. *J. Biol. Chem.* **285,** 13223–13232
37. Yang, T. T., Suk, H. Y., Yang, X., Olabisi, O., Yu, R. Y., Durand, J., Jelicks, L. A., Kim, J. Y., Scherer, P. E., Wang, Y., Feng, Y., Rossetti, L., Graef, I. A., Crabtree, G. R., and Chow, C. W. (2006) Role of transcription factor NFAT in glucose and insulin homeostasis. *Mol. Cell. Biol.* **26,** 7372–7387